

Supplementary information for

## **Flexible-Spacer Incorporated Polymer Donors Enable Superior Blend Miscibility for High-Performance and Mechanically-Robust Polymer Solar Cells**

*Jin-Woo Lee,<sup>†,a</sup> Dahyun Jeong,<sup>†,a</sup> Dong Jun Kim,<sup>b</sup> Tan Ngoc-Lan Phan,<sup>a</sup> Jin Su Park,<sup>a</sup> Taek-Soo Kim<sup>b</sup> and Bumjoon J. Kim<sup>\*,a</sup>*

<sup>a</sup>Department of Chemical and Biomolecular Engineering, <sup>b</sup>Department of Mechanical Engineering, Korea Advanced Institute of Science and Technology (KAIST), Daejeon 34141, Republic of Korea

\* All correspondence should be addressed to B. J. K. (E-mail: [bumjoonkim@kaist.ac.kr](mailto:bumjoonkim@kaist.ac.kr))

**KEYWORDS:** polymer solar cell; polymer donor; non-fullerene small-molecule acceptor; mechanical robustness; high efficiency.

## Table of Contents

### Additional experiments

#### Supplementary Figures

**Fig. S1** Collected  $^1\text{H}$  NMR spectra of PM6-CX  $P_{\text{DS}}$ .

**Fig. S2** (a) UV-vis absorption spectra of the  $P_{\text{DS}}$  and Y7 acceptor in film state. (b) Cyclic voltammograms and (c) energy diagrams for the  $P_{\text{DS}}$ .

**Fig. S3** Temperature-dependent UV-Vis absorption spectra for the pristine  $P_{\text{DS}}$  in solutions.

**Fig. S4**  $J_{\text{ph}}$  vs.  $V_{\text{eff}}$  curves for the  $P_{\text{D}}$ :Y7 blends.

**Fig. S5** AFM height images of the  $P_{\text{D}}$ :Y7 blends.

**Fig. S6** DSC thermograms of (a) PM6-CX  $P_{\text{DS}}$  and (b) Y7 for the 1<sup>st</sup> heating cycle.

**Fig. S7** Normalized UV-vis absorption spectra of the  $P_{\text{D}}$ :Y7 blends in film state.

**Fig. S8** GIXS linecut profiles of the pristine  $P_{\text{DS}}$  in the (a) IP and (b) OOP directions, (c)  $L_{\text{c}}$  values of the (100) scattering peaks for both IP and OOP directions depending on the  $P_{\text{DS}}$ ; (d)  $L_{\text{c}}$  values extracted from (100) scattering peaks at different polar angles.

**Fig. S9** 2D GIXS images of the pristine  $P_{\text{DS}}$ .

**Fig. S10** GIXS linecut profiles for the  $P_{\text{D}}$ :Y7 blends in the (a) IP and (b) OOP directions.

**Fig. S11** (a) Sample structure for the DCB tests; (b)  $G_{\text{c}}$  values of the blend films depending on the  $P_{\text{DS}}$ .

**Fig. S12** Load vs. displacement curves from the DCB tests for the blends with (a) PM6, (b) PM6-C5, (c) PM6-C10, (d) PM6-C20 and (e) PM6-C30  $P_{\text{DS}}$ .

**Fig. S13** (a) Experimental setup for the bending tests for the flexible devices, and (b) picture of the flexible devices.

**Fig. S14** (a)  $J$ - $V$  curves of the flexible devices without bendings; (b) normalized PCE vs. bending cycles of the  $P_{\text{D}}$ :Y7 blends.

#### Supplementary Tables

**Table S1** SCLC mobilities and thickness information for the  $P_{\text{D}}$ :Y7 blends.

**Table S2**  $\lambda_{\text{max}}$  values in the lower energy band measured from UV-Vis absorption spectroscopy of the blend films.

**Table S3** PCE and COS values of the binary PSC systems using SMA or SMA-polymerized acceptor in other works and this work.

**Table S4** Photovoltaic parameters of the flexible devices.

**Table S5** PCE values of the flexible devices depending on the bending cycles.

**Materials:** 4,8-Bis(5-(2-ethylhexyl)-4-fluorothiophen-2-yl)benzo[1,2-b:4,5-b']dithiophene-2,6-diyl)bis(trimethylstannane) (BDT monomer), 1,3-bis(5-bromothiophen-2-yl)-5,7-bis(2-ethylhexyl)benzo[1,2-c:4,5-c']dithiophene-4,8-dione (BDD monomer) were purchased from *SunaTech* Incorporation. The FS unit, 1,10-bis(5-bromothiophen-2-yl)decane, was synthesized by the method reported in the literature.<sup>1</sup> Y7 SMA was purchased from *Derthon*. 2,9-bis(3-((3-(dimethylamino)propyl)amino)propyl)anthra[2,1,9-*def*:6,5,10-*d'ef'*]diisoquinoline-1,3,8,10(2*H*,9*H*)-tetraone (PDINN) interlayer was synthesized by following the method in the previous report.<sup>2</sup> All other materials including catalysts were purchased from *Sigma Aldrich*.

**Fabrication of polymer solar cell (PSC):** The PSC device structure was indium tin oxide (ITO)/poly(3,4-ethylenedioxythiophene:polystyrene sulfonic acid) (PEDOT:PSS, AI4083 from Heraeus)/active layer/PDINN/Ag. ITO-coated glass substrates were washed by ultrasonication with acetone and isopropyl alcohol, and dried in an oven at 80 °C. The washed ITO-coated glass was plasma-treated for 10 min and PEDOT:PSS solution was spin-casted (3000 rpm, 30 s). Then, the substrates were thermally annealed (165 °C, 20 min) and moved into a glove-box. The bulk-heterojunction (BHJ) solutions with optimal conditions (20 mg mL<sup>-1</sup> in chlorobenzene, donor:acceptor = 1:1 and 1 vol% of 1-chloronaphthalene) were spin-coated onto the substrates (2000 rpm, 20 s), and baked at 100 °C for 5 min. Next, the PDINN solution (1 mg mL<sup>-1</sup> in methanol) was casted onto the BHJ layer (3000 rpm, 20 s) and top electrode (Ag, 120 nm) was thermally deposited. The photoactive area for PSC measurement was 0.164 cm<sup>2</sup>. The results of more than ten PSC devices were collected for each active system and the average/maximum photovoltaic parameters of the data are presented in **Table 2** to determine data reliability.

***Fabrication of flexible polymer solar cell (FPSC):*** The device fabrication procedures were based on the previous literature.<sup>3</sup> We used thermoplastic polyurethane (TPU) as the substrate because it has high transmittance and bendability. For the bottom electrode, we used PEDOT:PSS (Heraeus Clevios™ PH1000) to replace ITO and included additives to enhance the properties of the PEDOT:PSS. In detail, 5 vol% of dimethyl sulfoxide (DMSO) for better electrical properties, 2 vol% polyethylene glycol (PEG) for better mechanical properties, and 0.5 vol% of Zonyl fluorosurfactant (Zonyl FS-30) as a dopant were added into the PEDOT:PSS solution. The rest of the devices including active layer, electron transporting layer, and electrode were fabricated following the same processes with the PSC fabrication.

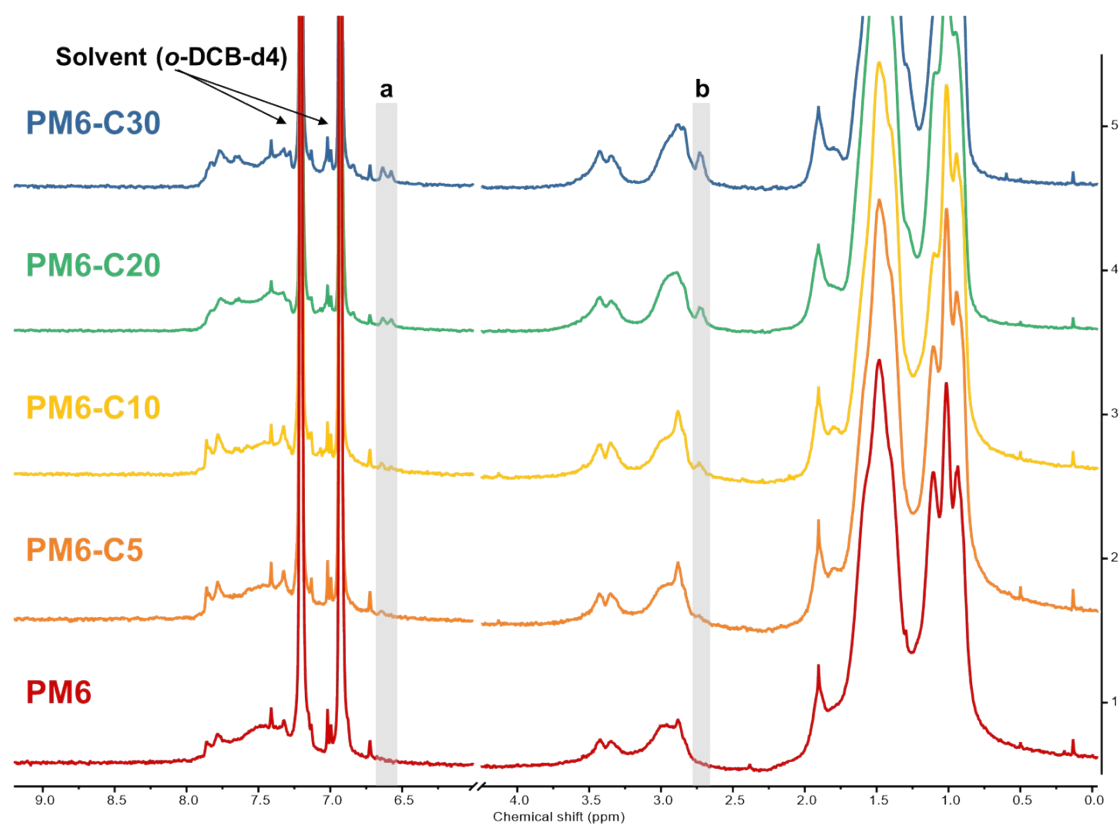
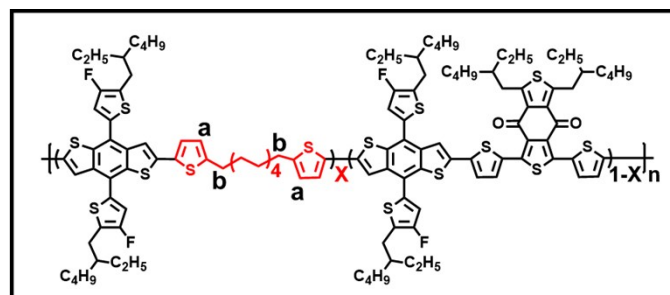


**Fig. S1** Collected  $^1\text{H}$  NMR spectra of PM6-CX  $P_{\text{Ds}}$ .

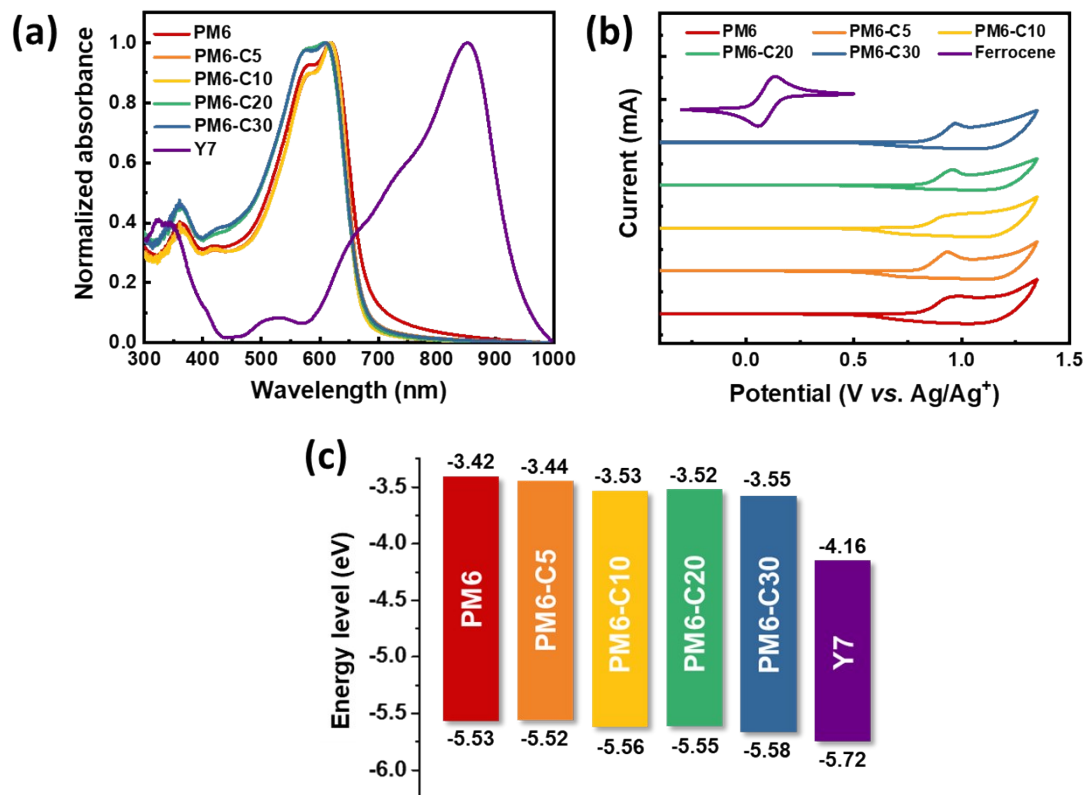


**Fig. S2** (a) UV-vis absorption spectra of the  $P_D$ s and Y7 acceptor in film state. (b) Cyclic voltammograms and (c) energy diagrams for the  $P_D$ s in this study.

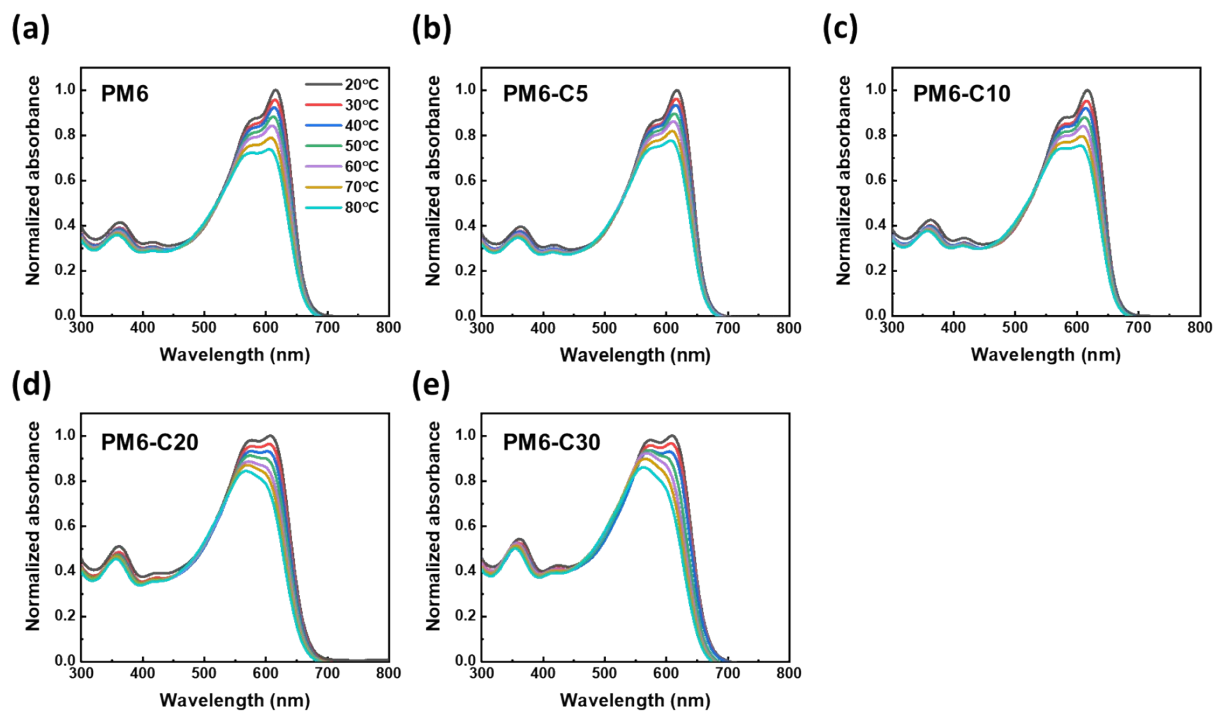


**Fig. S3** Temperature-dependent UV-Vis absorption spectra for the pristine  $P_{DS}$  in chlorobenzene solutions.

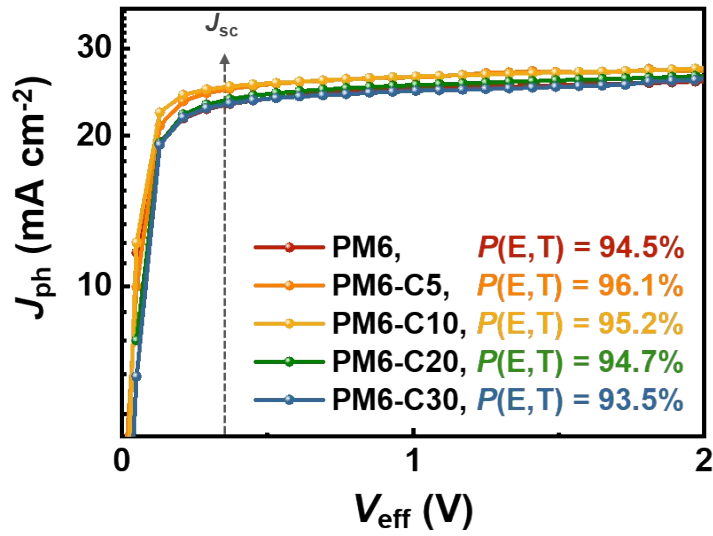


**Fig. S4**  $J_{ph}$  vs.  $V_{eff}$  curves for the  $P_D:Y7$  blends.

**Table S1** SCLC mobilities and thickness information for the  $P_D:Y7$  blends.

$P_D$	$\mu_h$ (cm <sup>2</sup> V <sup>-1</sup> s <sup>-1</sup> )	$\mu_e$ (cm <sup>2</sup> V <sup>-1</sup> s <sup>-1</sup> )	Thickness (nm) <sup>a</sup>
PM6	$1.6 \times 10^{-4}$	$2.1 \times 10^{-4}$	107
PM6-C5	$4.0 \times 10^{-4}$	$2.9 \times 10^{-4}$	115
PM6-C10	$3.6 \times 10^{-4}$	$2.0 \times 10^{-4}$	110
PM6-C20	$8.4 \times 10^{-5}$	$7.6 \times 10^{-5}$	121
PM6-C30	$5.3 \times 10^{-5}$	$6.0 \times 10^{-5}$	118

<sup>a</sup>Thicknesses of the blend films are same as those in PSC fabrication.



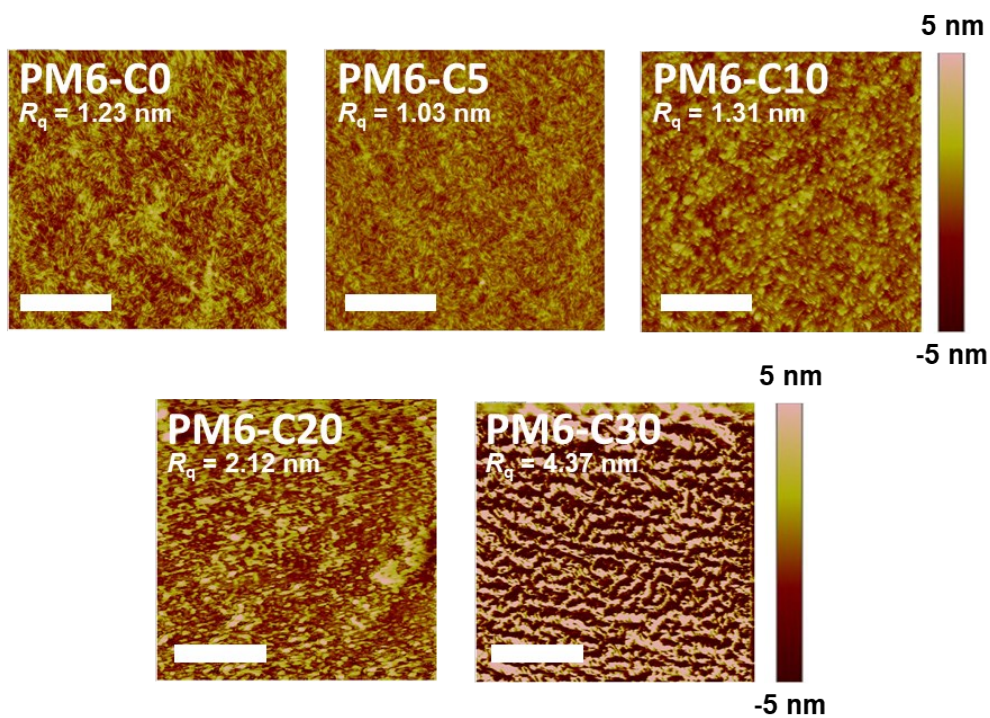


**Fig. S5** AFM height images of the  $P_D$ :Y7 blends (scale bars are  $1 \mu\text{m}$ ).

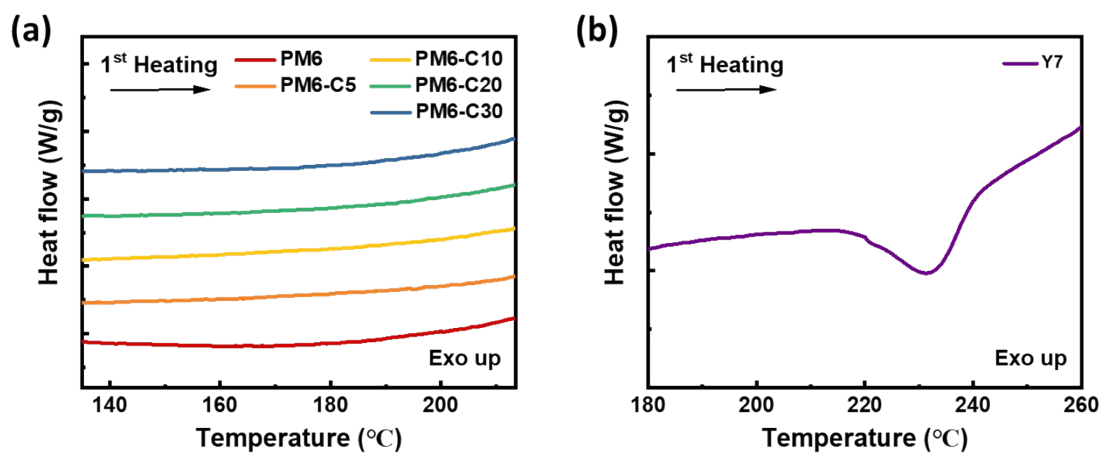


**Fig. S6** DSC thermograms of (a) PM6-CX  $P_D$ s and (b) Y7 for the 1<sup>st</sup> heating cycle.

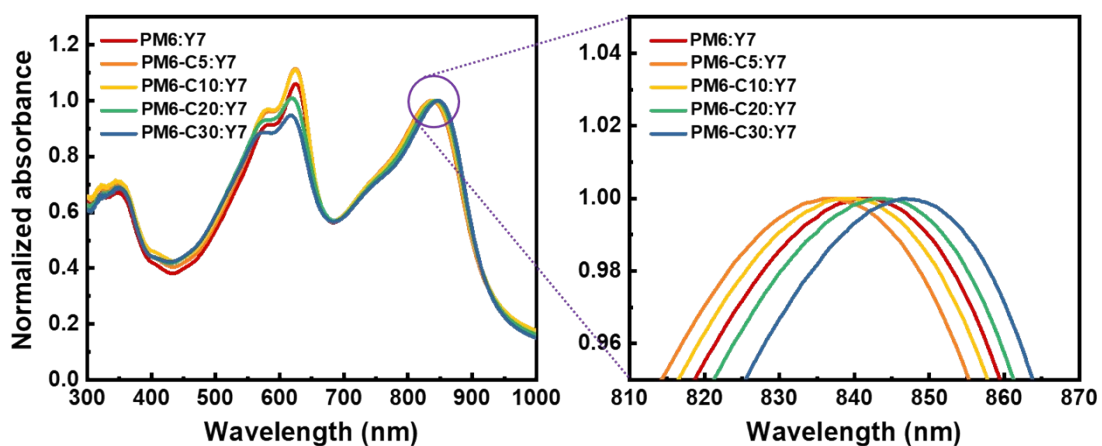


**Fig. S7** Normalized UV-vis absorption spectra of the  $P_D$ :Y7 blends in film state.

**Table S2**  $\lambda_{\max}$  values in the lower energy band measured from UV-Vis absorption spectroscopy of the blend films.

$P_D$	$\lambda_{\max}$ (nm)
<b>PM6-C0</b>	842
<b>PM6-C5</b>	837
<b>PM6-C10</b>	838
<b>PM6-C20</b>	843
<b>PM6-C30</b>	847

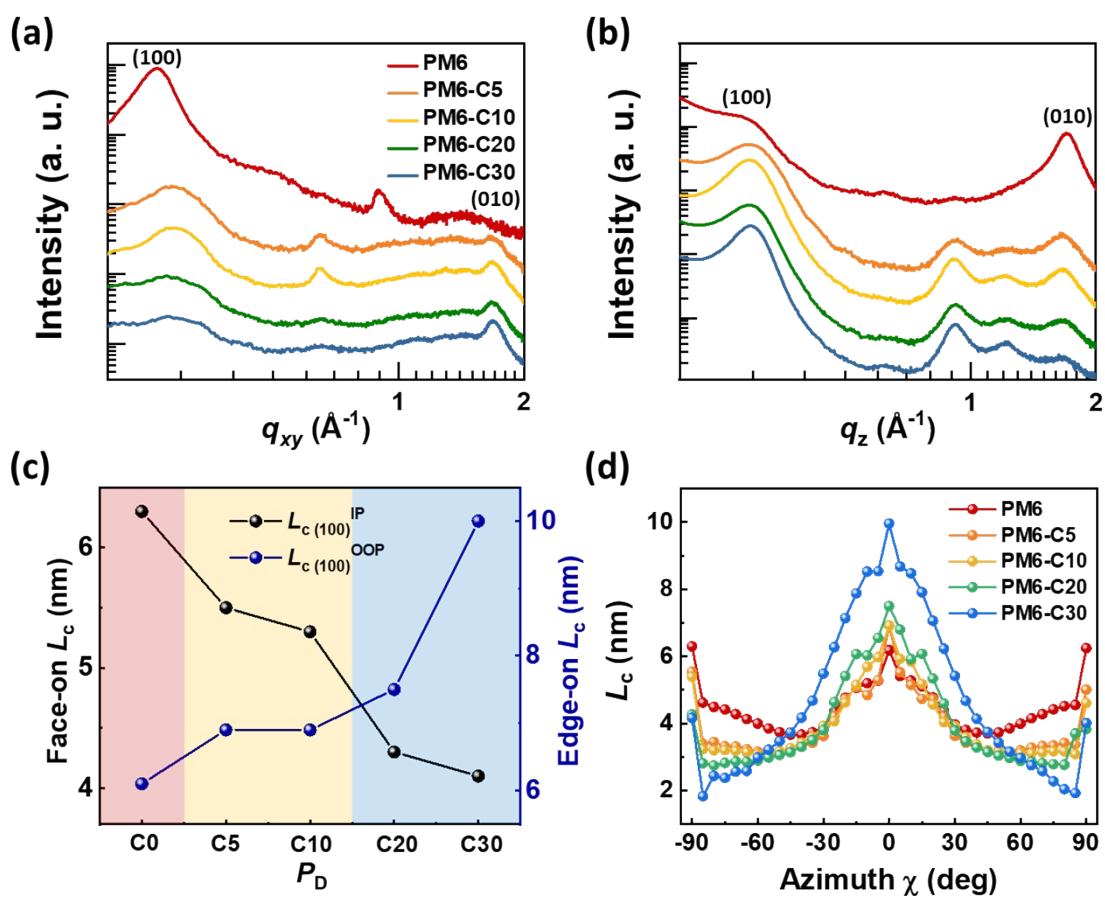


**Fig. S8** GIXS linecut profiles of the pristine  $P_D$ s in the (a) IP and (b) OOP directions; (c) coherence length ( $L_c$ ) values of the (100) scattering peaks for both IP (face-on) and OOP (edge-on) directions depending on the  $P_D$ s; (d)  $L_c$  values extracted from (100) scattering peaks at different polar angles.

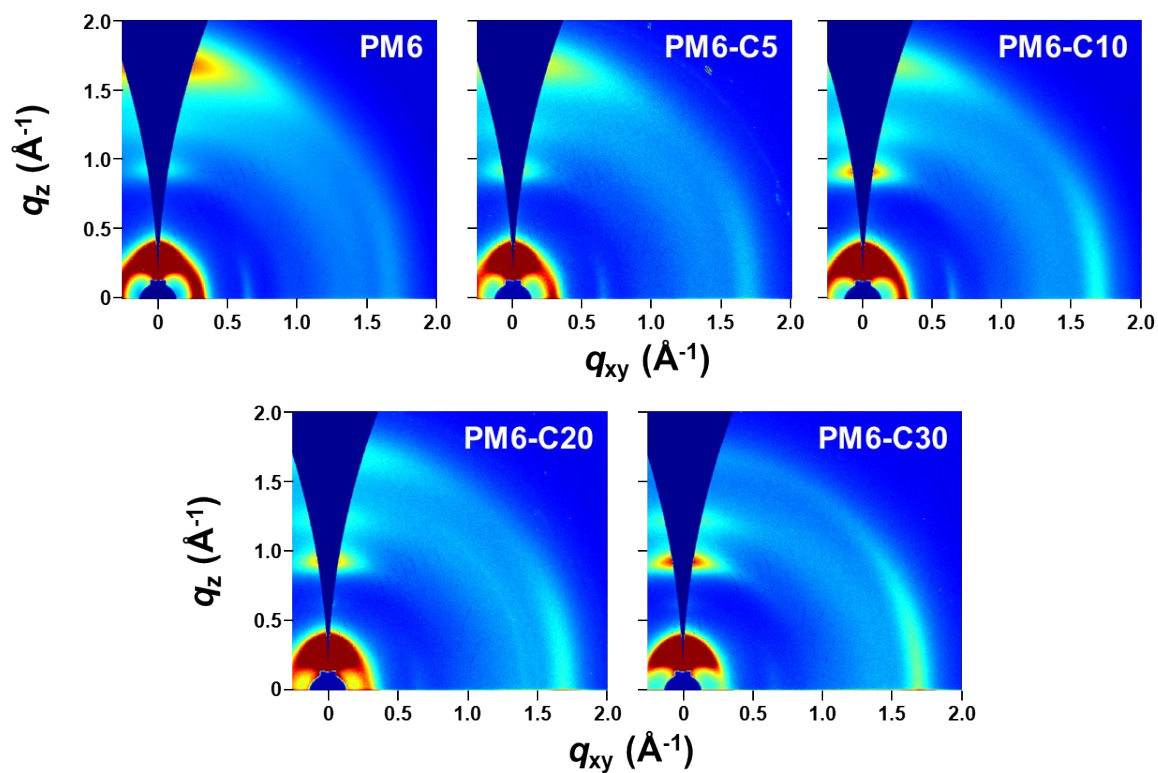


Fig. S9 2D GIXS images of the pristine  $P_D$ s.

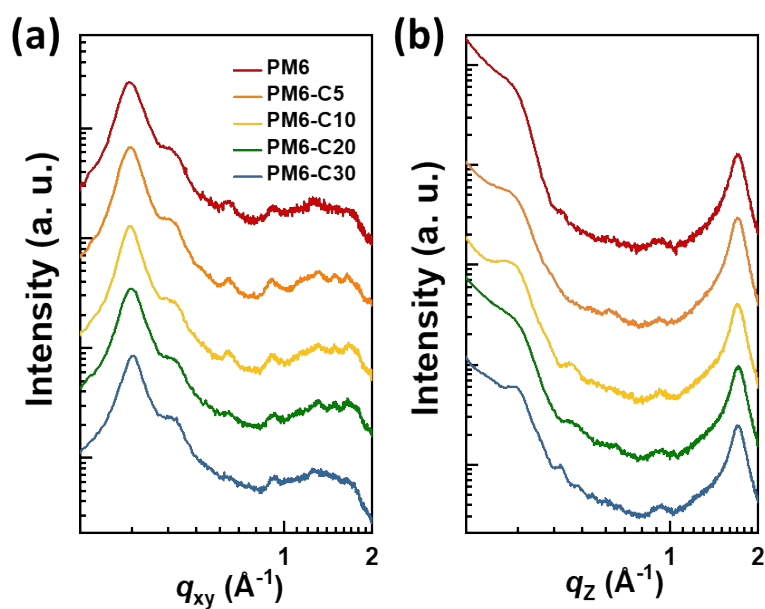
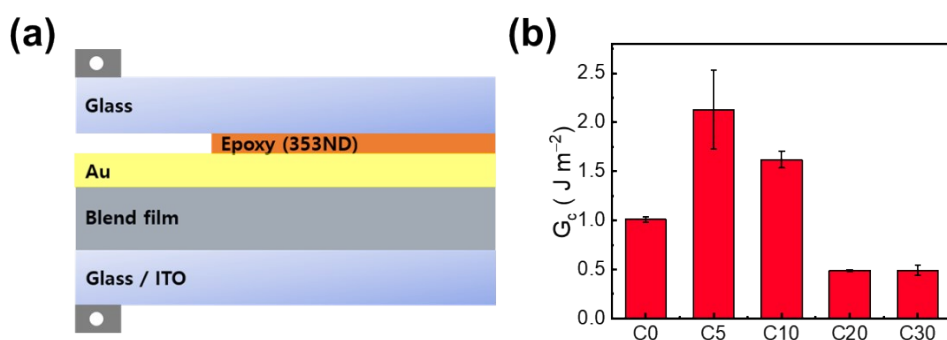
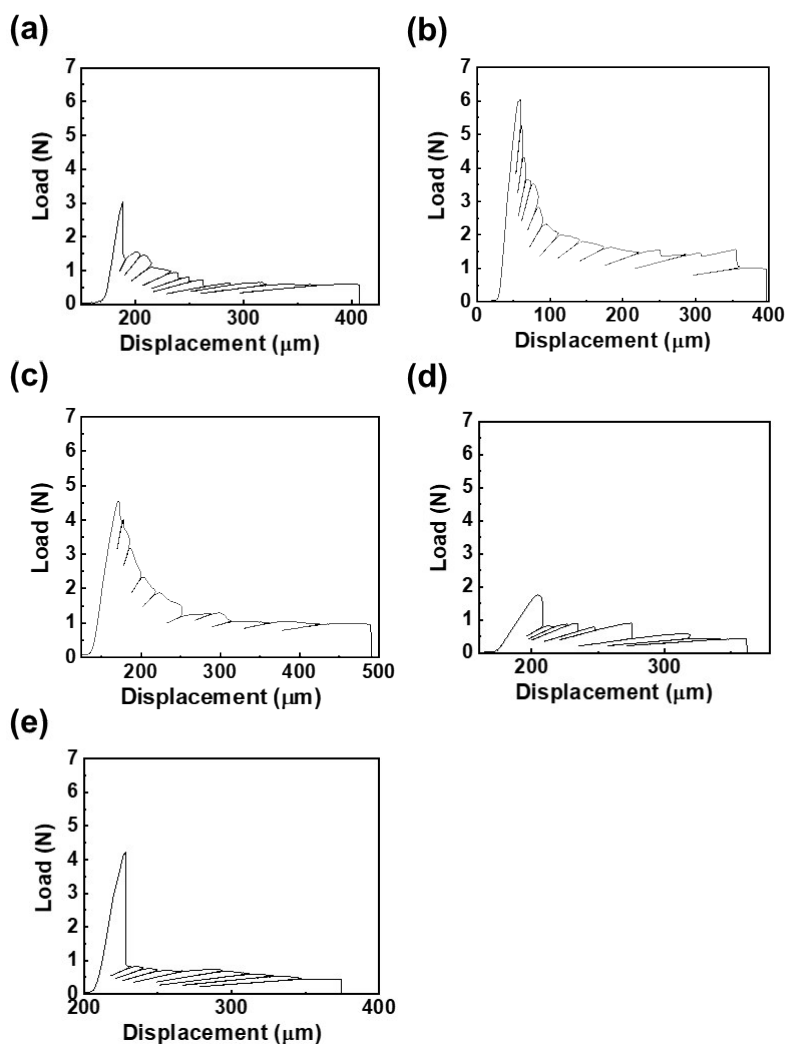


Fig. S10 GIXS linecut profiles for the  $P_D:Y7$  blends in the (a) IP and (b) OOP directions.



**Fig. S11** (a) Sample structure for the DCB tests; (b)  $G_c$  values of the blend films depending on the  $P_{DS}$ .



**Fig. S12** Load vs. displacement curves from the DCB tests for the blends with (a) PM6, (b) PM6-C5, (c) PM6-C10, (d) PM6-C20 and (e) PM6-C30  $P_{DS}$ .

**Table S3** PCE and COS values of the binary PSC systems using SMA or SMA-polymerized acceptor in other works and this work.<sup>4-12</sup>

<b>Blend</b>	<b>PCE<sub>max</sub> (%)</b>	<b>COS (%)<sup>a</sup></b>	<b>Reference</b>
PM6:IDIC16	4.9	1.4	3
PM6:PF2-DTC	8.3	11.3	3
PM6:PF2-DTSi	10.8	8.6	3
PM6:PF2-DTGe	8.1	6.7	3
PTB7:PC <sub>71</sub> BM (1:1.5)	0.3	2.1	4
PTB7:PC <sub>71</sub> BM (1:1)	0.1	4.3	4
PBDTTPD:PC <sub>61</sub> BM	6.1	0.1	5
PTB7-Th:FOIC (BHJ)	11.0	3.1	6
PTB7-Th:FOIC (P-i-N)	12.0	11.5	6
PTB7-Th:PC <sub>71</sub> BM	6.0	1.1	7
PTB7-Th:ITIC	6.4	3.4	7
PTB7-Th:P-15K	3.1	6.0	7
PTB7-Th:P-20K	3.4	11.2	7
PTB7-Th:PC <sub>71</sub> BM	8.4	1.1	8
PBDB-T:Y5-2BO	7.0	2.3	9
PBDB-T:P(BDT2BOY5-H)	8.8	19.3	9
PBDB-T:P(BDT2BOY5-F)	9.8	16.7	9
PBDB-T:P(BDT2BOY5-Cl)	11.1	15.9	9
PM6:Y6	15.4	5.8	10
PBDB-T:PYT (BHJ)	14.1	8.5	11
PBDB-T:PYT (LbL)	15.2	10.5	11
PM6-C5:Y7	16.7	12.1	This work

<sup>a</sup> The presented COSs stand for the values measured by pseudo free-standing tensile method.

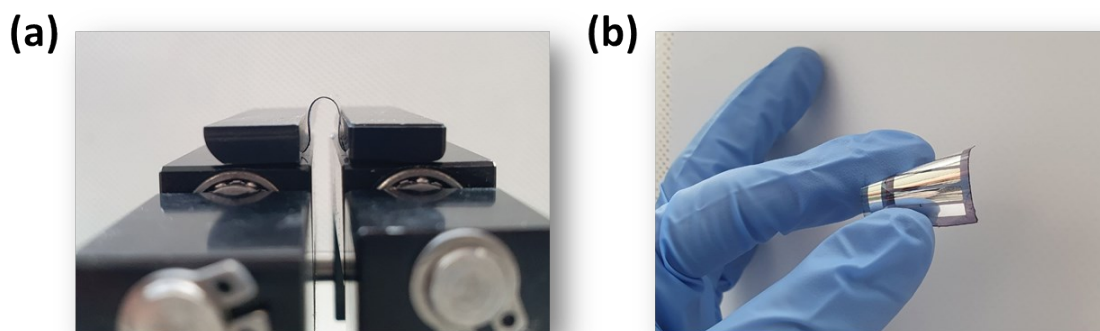


**Fig. S13** (a) Experimental setup for the bending tests for the flexible devices, and (b) picture of the flexible devices.

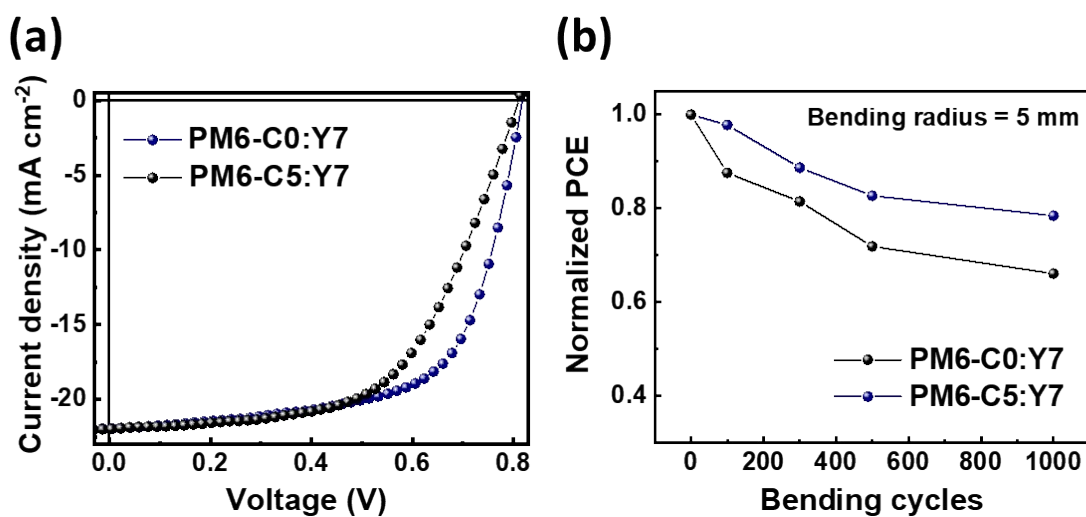


**Fig. S14** (a)  $J$ - $V$  curves of the flexible devices without bendings; (b) normalized PCE vs. bending cycles of the  $P_D$ :Y7 blends.

**Table S4** Photovoltaic parameters of the flexible devices (without bending).

$P_D$	$V_{oc}$ (V)	$J_{sc}$ (mA cm <sup>-2</sup> )	FF	PCE (%)
PM6-C0	0.81	21.99	0.58	10.29
PM6-C5	0.82	21.97	0.65	11.64

**Table S5** PCE values of the flexible devices depending on the bending cycles.

<b><math>P_D</math></b> \ <b>Cycle</b>	<b>0</b>	<b>200</b>	<b>500</b>	<b>1000</b>	<b>1500</b>
<b>PM6-C0</b>	10.29	9.01	8.39	7.40	6.81
<b>PM6-C5</b>	11.64	11.39	10.32	9.63	9.14



## References

1. B. C. Schroeder, Y. C. Chiu, X. D. Gu, Y. Zhou, J. Xu, J. Lopez, C. Lu, M. F. Toney and Z. N. Bao, *Adv. Electron. Mater.*, 2016, **2**, 1600104.
2. J. Yao, B. B. Qiu, Z. G. Zhang, L. W. Xue, R. Wang, C. F. Zhang, S. S. Chen, Q. J. Zhou, C. K. Sun, C. Yang, M. Xiao, L. Meng and Y. F. Li, *Nat. Commun.*, 2020, **11**, 2726.
3. J.-W. Lee, N. Choi, D. Kim, T. N.-L. Phan, H. Kang, T.-S. Kim and B. J. Kim, *Chem. Mater.*, 2021, **33**, 1070-1081.
4. Q. P. Fan, W. Y. Su, S. S. Chen, W. Kim, X. B. Chen, B. Lee, T. Liu, U. A. Mendez-Romero, R. J. Ma, T. Yang, W. L. Zhuang, Y. Li, Y. W. Li, T. S. Kim, L. T. Hou, C. Yang, H. Yan, D. H. Yu and E. G. Wang, *Joule*, 2020, **4**, 658-672.
5. J. H. Kim, J. Noh, H. Choi, J. Y. Lee and T. S. Kim, *Chem. Mater.*, 2017, **29**, 3954-3961.
6. T. Kim, J. H. Kim, T. E. Kang, C. Lee, H. Kang, M. Shin, C. Wang, B. W. Ma, U. Jeong, T. S. Kim and B. J. Kim, *Nat. Commun.*, 2015, **6**, 8547.
7. Y. L. Wang, Q. L. Zhu, H. B. Naveed, H. Zhao, K. Zhou and W. Ma, *Adv. Energy Mater.*, 2020, **10**, 1903609.
8. J. Choi, W. Kim, S. Kim, T. S. Kim and B. J. Kim, *Chem. Mater.*, 2019, **31**, 9057-9069.
9. W. Lee, J. H. Kim, T. Kim, S. Kim, C. Lee, J. S. Kim, H. Ahn, T. S. Kim and B. J. Kim, *J. Mater. Chem. A*, 2018, **6**, 4494-4503.
10. J. W. Lee, C. Sun, B. S. Ma, H. J. Kim, C. Wang, J. M. Ryu, C. Lim, T. S. Kim, Y. H. Kim, S. K. Kwon and B. J. Kim, *Adv. Energy Mater.*, 2021, **11**, 2003367.
11. J. H. Han, F. Bao, D. Huang, X. C. Wang, C. M. Yang, R. Q. Yang, X. G. Jian, J. Y. Wang, X. C. Bao and J. H. Chu, *Adv. Funct. Mater.*, 2020, **30**, 2003654.
12. Q. Wu, W. Wang, Y. Wu, Z. Chen, J. Guo, R. Sun, J. Guo, Y. Yang and J. Min, *Adv. Funct. Mater.*, 2021, **31**, 2010411.